Vol.67: e24230669, 2024
https://doi.org/10.1590/1678-4324-2024230669
ISSN 1678-4324 Online Edition

BABT
Brazilian Archives of Biology and Technology

Article - Engineering, Technology and Techniques

Development of a Low-Energy Mobile Current Waveform Impulse Generator for Application in Low Voltage Surge Arresters

Tiago Goncalves Zacarias[1]
https://orcid.org/0000-0002-0156-6546

Frederico de Oliveira Assunção[1]
https://orcid.org/0000-0002-5304-8628

Rafael Martins[2]
https://orcid.org/0000-0002-0776-2978

Levy Ely de Lacerda de Oliveira[1]
https://orcid.org/0000-0001-9052-5801

Carlos Eduardo Xavier[2]
https://orcid.org/0000-0002-1144-7276

Carlos Eduardo Teixeira[1]
https://orcid.org/0000-0003-3399-1878

Júlio Cezar Oliveira Castioni[2]
https://orcid.org/0000-0002-1144-9247

Luiz Eduardo Borges da Silva[1]
https://orcid.org/0000-0003-2298-1017

Germano Lambert-Torres[1]*
https://orcid.org/0000-0003-3789-4696

Erik Leandro Bonaldi[1]
https://orcid.org/0000-0003-4350-9248

[1]Instituto Gnarus, Itajubá, Minas Gerais, Brasil; [2]COPEL Geração e Transmissão, Curitiba, Paraná, Brasil.

Editor-in-Chief: Alexandre Rasi Aoki
Associate Editor: Alexandre Rasi Aoki

Received: 28-Jun-2023; Accepted: 12-Sep-2023

*Correspondence: germanoltorres@gmail.com; Tel.: +55-35- 3622-0132 (G.L.T.).

HIGHLIGHTS

- Development of a laboratory with a low-energy, mobile current waveform impulse generator.
- The goal is of this laboratory is for conducting aging tests on low-voltage zinc oxide surge arresters.
- The current waveform impulses are sufficient to induce degradation in the electrical parameters of the tested surge arresters.
- Results of testing performed on new ZnO surge arrester samples.

Abstract: Surge arresters are at the forefront of protection against voltage surges. The loss of the protective effect of surge arresters imposes accidents and unplanned shutdowns on the power system. It directly affects the interruption of power supplies and imposes fines on service providers. Monitoring and diagnostics in the lightning rod field require studies and work that present the degradation behaviour of surge arresters to help develop and improve existing techniques. This paper presents the development of a laboratory with a low-energy, mobile current waveform impulse generator. It allows for conducting aging tests by applying discharges to low-voltage zinc oxide surge arresters used in the energy distribution sector. Samples of surge arresters were subjected to the discharges produced by the developed generator, and they exhibited degradation, thus showing asymmetry between the positive and negative half-cycles of leakage current.

Keywords: Metal oxide varistor; impulse current discharge; accelerated ageing; surge arrester degradation.

INTRODUCTION

The electrical system comprises various equipment and devices, each performing its function for the proper operation and reliability of the power system. The electrical system as a whole is exposed to multiple threats, particularly atmospheric discharges, which are unpredictable. To protect the entire system, including its equipment and devices, the use of surge arresters is widely applied [1-3].

Metal-oxide surge arresters (MOSAs) are connected to the system in parallel with what is desired to be protected. They are subjected to constant power dissipation, temporary overvoltage, and environmental conditions such as gas pollution, dust, and humidity. According to [4], 60% of failures in surge arresters in China are caused by moisture penetration into the enclosure. The highest incidence occurs in porcelain surge arresters.

The exposures of surge arresters to environmental aggressors affect their reliability. Over the years, other monitoring and diagnostic methodologies have been developed and improved. There are techniques classified as online, which do not require lightning rod shutdown, and offline, which require the removal of the lightning rod [5]. The development and validation of these methodologies are carried out in controlled environments (laboratories), requiring ways to induce aging in study samples in the shortest possible time. The literature presents studies aimed at understanding the behaviour and changes caused in surge arresters through the application of laboratory tests, as seen in [6-9], which form the basis for future work in monitoring and diagnostics.

Understanding how degradations occur and how each type of aggressor affects the electrical properties of surge arresters is of great interest in the maintenance field. This knowledge enables the improvement and development of new methodologies for monitoring and diagnostics.

The existing laboratories for aging tests are excessively large and costly, especially for current impulse applications, which impose financial limitations and hinder their involvement in the field of lightning arrester monitoring and diagnostics. Therefore, it is necessary to develop more affordable equipment and methodologies, and one of the purposes of this article is to present an accessible solution that can be easily replicated.

This paper presents the development of a gapless metal-oxide surge arrester (MOSA) testing laboratory. It employs current impulse applications via a low-energy generator and moisture effects directly delivered to the surge arresters' internal disks. The following section explains the theoretical features required to comprehend the results reported in this paper, including a brief introduction to the operating principle of MOSAs and the technical terms discussed. After that, another section summarizes the primary substances that cause surge arrester deterioration. And then, a section describes the developed laboratory, equipment, and techniques. Finally, another section provides the results of testing performed on new ZnO surge arrester samples.

ZINC OXIDE SURGE ARRESTERS

Developed in the mid-1970s by Matsuoka and his research team, zinc oxide (ZnO) surge arresters exhibit excellent characteristics for applications in overvoltage protection. Its high nonlinearity [10], compared to its predecessor, silicon carbide (SiC), allowed for the development of new surge arrester structures without the need for gaps. Under normal operating conditions, the metal-oxide surge arrester (MOSA) behaves as an insulator, with only a few microamperes of current flowing [11]. In the presence of transients, it responds rapidly and enables the flow and drainage of high levels of electrical current (in the kiloampere range). After the transient is removed, it returns to its insulating state. Figure 1 shows the primary equivalent circuit of a metal oxide lightning arrestor.

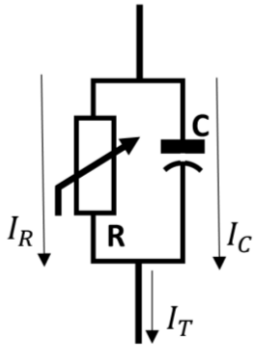

Figure 1. MOSA primary equivalent circuit [12].

Leakage current

Due to the removal of the gap in the surge arrester structure, there is the flow of electrical current through the surge arrester, known as leakage current, which is of low intensity under normal conditions. All currents are time-dependent. The currents shown in Figure 1 are the currents that flow through the varistor discs during their operation. Furthermore, according to [12-14], the resistive component increases with varistor degradation, while the capacitive component remains unchanged or undergoes minimal changes. The resistive component of the leakage current is sensitive to various types of degradation [15]. It is the most widely applied condition monitoring method in the literature [16].

Nonlinearity

The high nonlinearity characteristic of ZnO varistors is a result of their microstructure. According to [17], the homogeneity of the microstructure and the grain size are essential factors in determining the varistor's characteristics. The nonlinearity property of the varistor is due to the segregation layer formed by additives, where a depletion layer exists.

This behaviour has a coefficient that can be obtained from the parameters of the "*VxI*" curve. The coefficient of nonlinearity can be obtained using equation (1).

$$\alpha = \frac{log\left(\frac{I_2}{I_1}\right)}{log\left(\frac{V_2}{V_1}\right)} \quad (1)$$

Where α is the coefficient of nonlinearity, I_2 and I_1 are current values at points on the VxI curve (Figure 2), and V_2 and V_1 are the corresponding voltages for those currents.

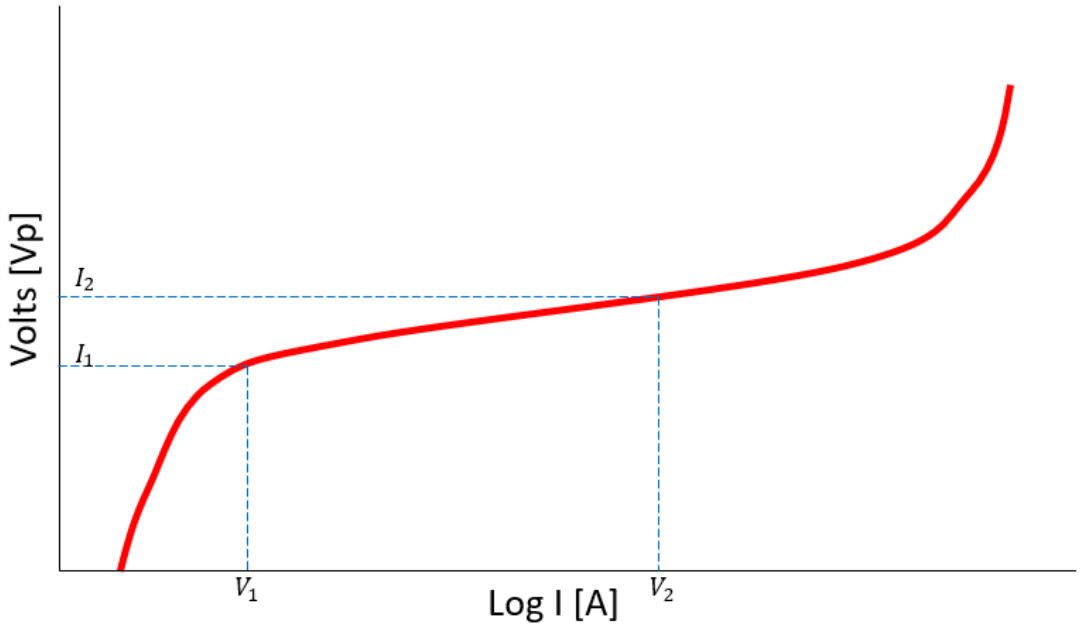

Figure 2. Typical VxI curve of ZnO

DEGRADATION AND FAILURE OF METAL OXIDE LIGHTNING ARRESTER

Surge arresters are subjected to constant power dissipation, temporary overvoltage, and environmental conditions such as gas pollution, dust, and humidity. The causes of failures and loss of electrical characteristics of the varistor blocks can be attributed to the factors described below:

- Atmospheric discharges
- Temporary overvoltage
- External pollution of gases and Dust
- Bad sizing
- Moisture ingress

Reference [18] categorizes these factors into two types: electrical and non-electrical. Degradation resulting from non-electrical factors causes very slight changes in the "voltage-current" behaviour of zinc oxide surge arresters. These factors include humidity, temperature, wind speed, and solar radiation. Humidity, in particular, leads to an increase in the leakage current of the surge arrester.

Figure 3. Surge arrester damaged after failure in operation [19].

Atmospheric discharges

The damage caused to surge arresters due to lightning strikes is a common reason for their replacement. Due to their role in mitigating the effects of lightning strikes, surge arresters experience high energy applications in very short periods, resulting in total or partial loss of their protective capabilities.

According to [20], there are two types of damage: fault or degradation of the elements. Fault-type damages result in instant damage to the varistor elements, manifesting as destruction (Figure 3) or punctures and perforations (Figure 4). On the other hand, degradation damages affect the *V-I* characteristic of the varistor blocks, which can eventually lead to a fault.

Figure 4. Damage caused by lightning [21].

Temporary overvoltage

Continuous exposure to alternating voltage imposes a constant current flow through the ZnO surge arrester, resulting in energy dissipation. This dissipation increases the operating temperature of the varistor blocks, and as long as it remains within its thermal capabilities, it enables the functioning and reliability of equipment protection.

The degradation exhibited by the surge arrester when subjected to this transient situation is progressive and, in some cases, more critical, particularly when the duration exceeds several tens of seconds. In this second case, the surge arrester may enter a process of thermal runaway [22, 23], leading to a fault or failure.

The damages caused by surges, including lightning strikes, temporary overvoltages, and switching surges, result in the effects previously mentioned in a previous section.

External pollution by gases and dust

During its service life, the surge arrester is exposed to the accumulation of contaminants, dust, and humidity along its body. This uneven concentration alters the voltage distribution along the surge arrester's body, resulting in stress-induced degradation [24, 25]. Consequently, the leakage current flowing through the exterior surfaces increases and becomes part of the total leakage current of the surge arrester, thereby affecting leakage current monitoring methodologies. According to the manufacturer ABB [26], silicone polymer housings exhibit lower susceptibility to the effects of degradation caused by external contamination. The literature presents several studies that address the effect of pollution on the exterior of the enclosures [27-30].

Bad sizing

Indeed, inadequate planning and sizing of the surge protection system, including selecting inappropriate surge arresters, can lead to failures. The choice of the operating voltage level of the surge arrester is a crucial factor for its application. Under sizing can result in thermal runaway processes. The type of enclosure, whether polymer or porcelain, should be specified based on the environmental conditions in which the device is installed.

Moisture ingress

According to [1], the primary source of degradation in high-voltage equipment is moisture ingress, which causes deterioration of internal and external parts of the surge arrester. Exposure of contacts and electrodes initiates the process of oxidation (Figure 5) and internal partial discharges. The high moisture content combined with the elevated internal temperature of the surge arrester results in changes in the physical state of water molecules, known as condensation. It is the point where water accumulates in its liquid form, imposing an electric current and water flow on the ZnO blocks. In [31], a study on the effects of moisture penetration in low-voltage ZnO blocks is presented, where oxidation reactions occurred on the surfaces of the blocks.

The presence of moisture causes a decrease in the overall performance of the ZnO blocks. The increase in leakage current, especially its resistive component, directly affects electrical losses and heat generation in the surge arrester. The change in the system's thermal behaviour can result in the loss of thermal stability, where the surge arrester cannot dissipate all the heat generated to the surrounding environment. Considering the aggravating effects caused by moisture and how it can enhance other factors, its influence and impact on the lifespan of surge arresters are evident [32].

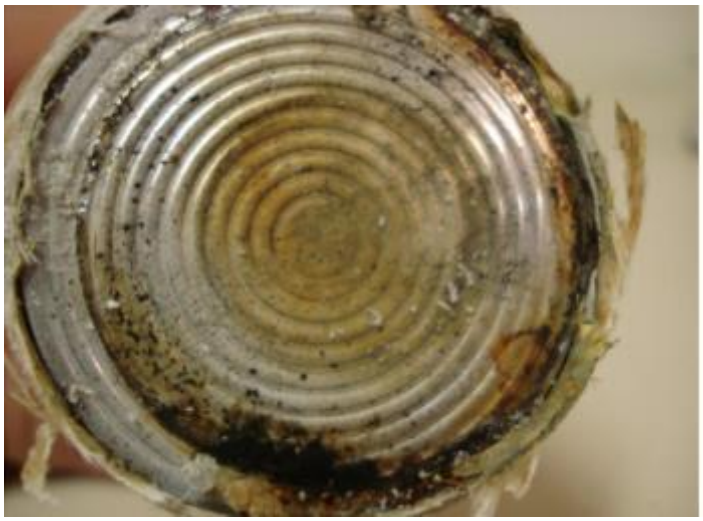

Figure 5. Metal oxide varistor block affected by moisture [33]

THEORETICAL BASIS

The impulse generator circuits can produce a high voltage level at their output for short periods of time. The standard IEC 60060-1 [34] defines the types of impulse waveforms and their characteristics.

Current impulse

The current waveform impulse is defined by the standard [34], which specifies three types of waveforms (Table 1 [34]). The parameters T_1 (front time) and T_2 (tail time) are defined, with variations of up to 10% of the standard values being accepted for each parameter (Figure 6).

Table 1. IEC 60060-1 impulse current waveforms.

Type	T_1[µs]	T_2[µs]
1	4	10
2	8	20
3	30	80

The standard curve includes the Undershoot effect, defined by the norm and limited to values not exceeding 20% of the peak value of the generated waveform.

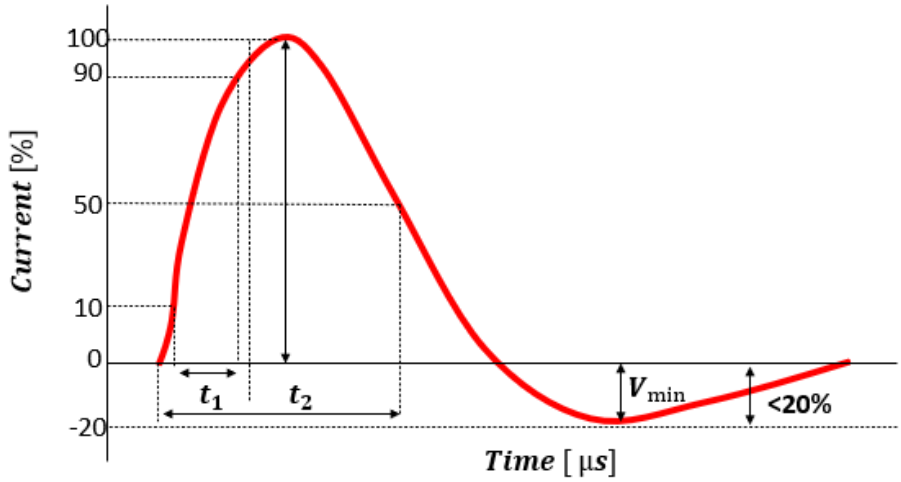

Figure 6. Impulse current wave parameters[34]

Wave conditioning circuit

To generate the current waveform impulse, the base circuit (Figure 7) was used, where the value of resistor *Rp* determines the tail time of the waveform, and *Rs* and *Cb* determine the front time of the waveform. The front time T_1 is obtained using the relationship given in equation (2), and T_2 can be determined using the connection shown in equation (3).

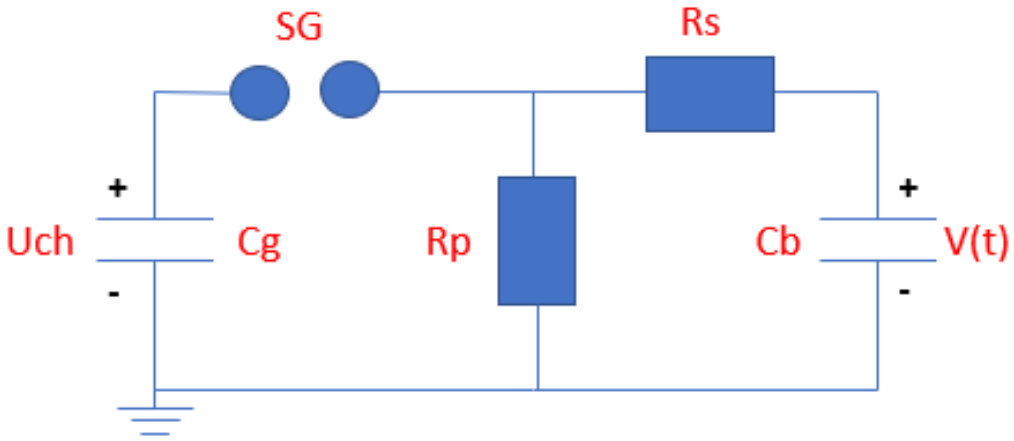

Figure 7. Current waveform impulse generator electric circuit – based on [35].

Where *Uch* Is the charging voltage; *Cg* is the capacitance of the generator; *SG* is the spark gap that defines the firing voltage; *Rp is* the parallel resistance, responsible for the tail time; *Rs* is the series resistance, responsible for the front; and *Cb* is the capacitance presented by the load.

$$T_1 = 3{,}25 R_s C_1$$
$$C_1 = \frac{(C_g \,.\, C_b)}{(C_g + C_b)} \quad (2)$$

$$T_2 = 0{,}693 R_p C_2 \quad (3)$$
$$C_2 = C_g + C_b$$

DEVELOPED LABORATORY

This section presents a mobile laboratory developed for the partial aging process. Detailed construction and technical information will be provided to enable the replication of the experiment. The laboratory, shown in Figure 8, is designed to apply up to 30 kV peak voltage with an energy of 0.1 kJ. It generates an 8/20 µs waveform, and modifying components in the waveform conditioning circuit can make adjustments.

Figure 8. Laboratory portable impulse current waveform low energy.

Electric diagram

The electrical diagram is presented in Figure 9, composed of a Marx generator [36]. The circuit is fed with direct voltage and provides a parallel association of capacitors, and series resistors allow different charging times for each capacitor. At the end of the charge, the last capacitor in the array reaches sufficient electrical potential to break the dielectric strength of the air and conduct it through the spark gaps. Conduction creates the path highlighted in red (Figure 9a) through which the capacitors are connected in series and discharged in the conditioning circuit (Figure 9b).

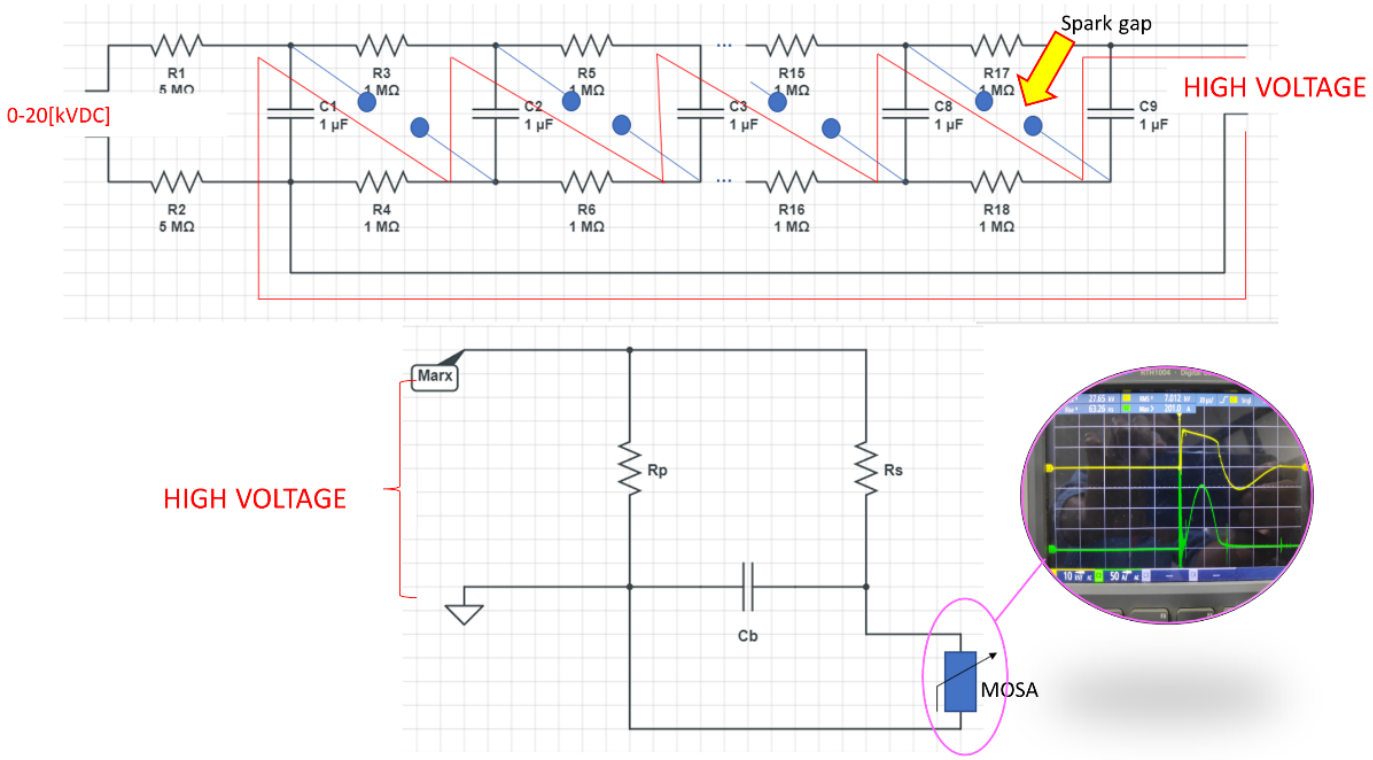

Figure 9. Impulse generator electrical diagram: a – Marx generator, b – Conditioning circuit.

Capacitors

The specifications of the capacitors shown in Figure 11, used for voltage boosting of the DC source and energy supply, are provided in Table 2. A series combination of 9 capacitors was used to achieve a voltage increase of 9 times. The capacitors need a high insulation rating, in this case, 5 kV.

Table 2. Technical data high voltage capacitors

Capacitance [µF]	Quantity	Association	Type	Temp [°C]
1	9	series	T	105

Resistors

The resistance values adopted for the conditioning circuit and Marx generator resistors are shown in Table 3. The resistors used in the waveform conditioning circuit are of the wire-wound type and exhibit inductive effects. For the high-voltage capacitor charging resistors, high-insulation carbon film resistors were used.

Table 3. Values of resistors used in electrical circuits

Resistance [Ω]	Quantity	Application	Type	Temp [°C]
1M	20	Capacitor R load	Metal film	105
100	1	Rp	Wirewound	400
4.7	2	Rs	Wirewound	400

Sphere gap

The sphere gap (Figure 10) was used due to its uniform electric field distribution. It was affixed on a Polyvinyl Chloride (PVC) structure to ensure high dielectric strength and prevent partial discharges.

The spheres have a diameter of 30mm and can be adjusted to change the spacing between them, allowing for the adjustment of discharge voltage levels.

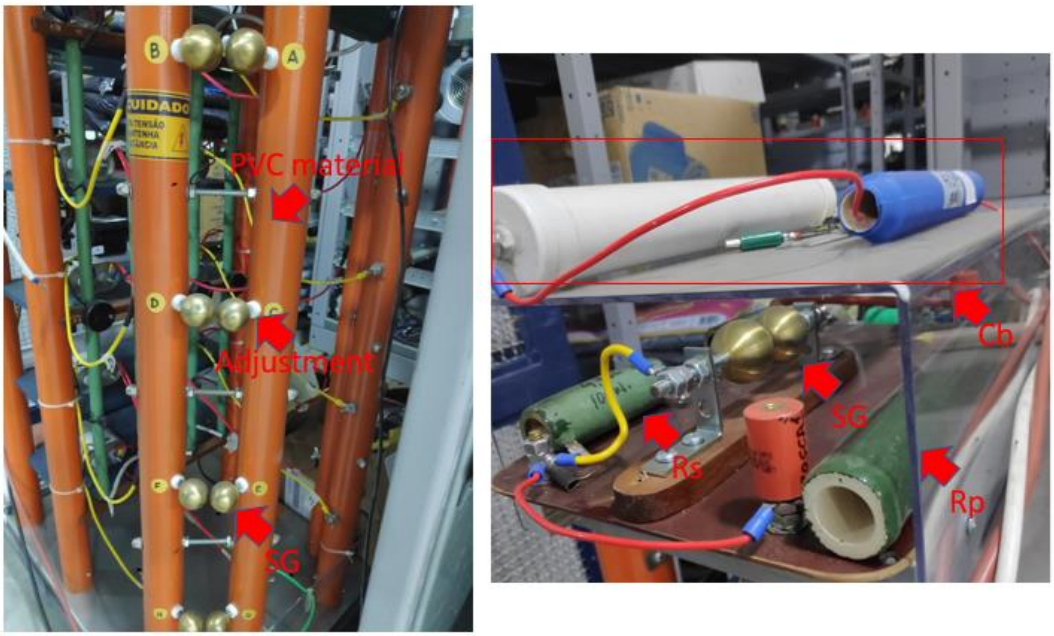

Figure 10. High voltage structure made of PVC material.

Power supply

The power supply was obtained using a potential transformer connected to a bridge of diodes (Figure 11). The specifications of the transformer are presented in Table 4.

Table 4. Power supply power transformer board datasheet

Frequency [Hz]	Transform ratio	S[VA]
60	1:120	500

Figure 11. Circuit based on the Marx generator.

RESULTS

The impulse waveform generator was tested in the laboratory along with new surge arresters. Three units of distribution-type surge arresters with a nominal voltage of 6[kV] and a nominal current of 10[kA] were tested. The yellow curve represents the voltage waveform, with flattening due to the capacitance of the surge arrester, while the green curve represents the discharge current. The residual values in the tested surge arresters were 19[kV] and 152[A] peak, as shown in Figure 12.

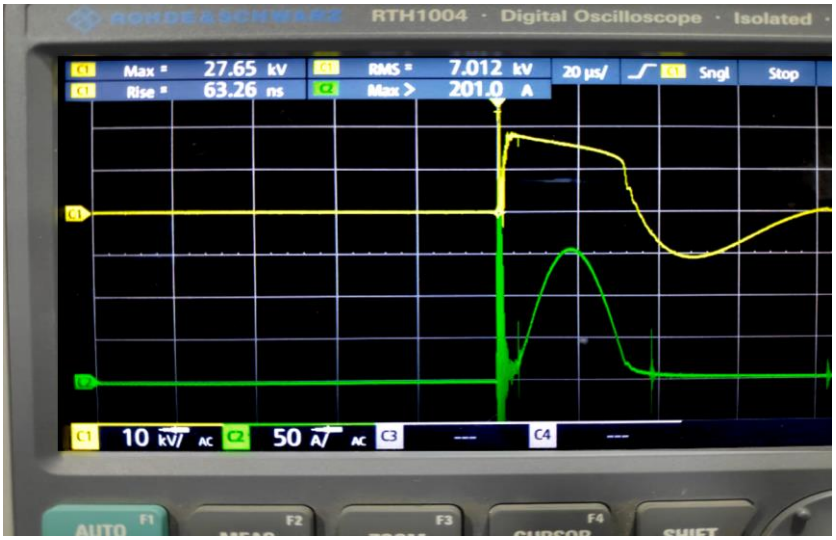

Figure 12. Impulse voltage and current waveforms.

The presence of asymmetry in the leakage current waveform is an indication of degradation. This asymmetry results from the polarization caused in the surge arresters due to the application of impulses, which can vary depending on the characteristics of the applied impulse waveform.

The voltage applied to the lightning arrester was measured to allow the extraction of the resistive leakage current, achieved by subtracting a virtual capacitive current considering only the 60Hz component. The observed effect was the polarization of the three samples (Figures 13-15), which directly impacts the VxI curve behavior. This type of effect occurs after subjecting the lightning arrester to atmospheric discharges, demonstrating the capability of the developed laboratory to induce degradation in low-voltage distribution-type lightning arresters.

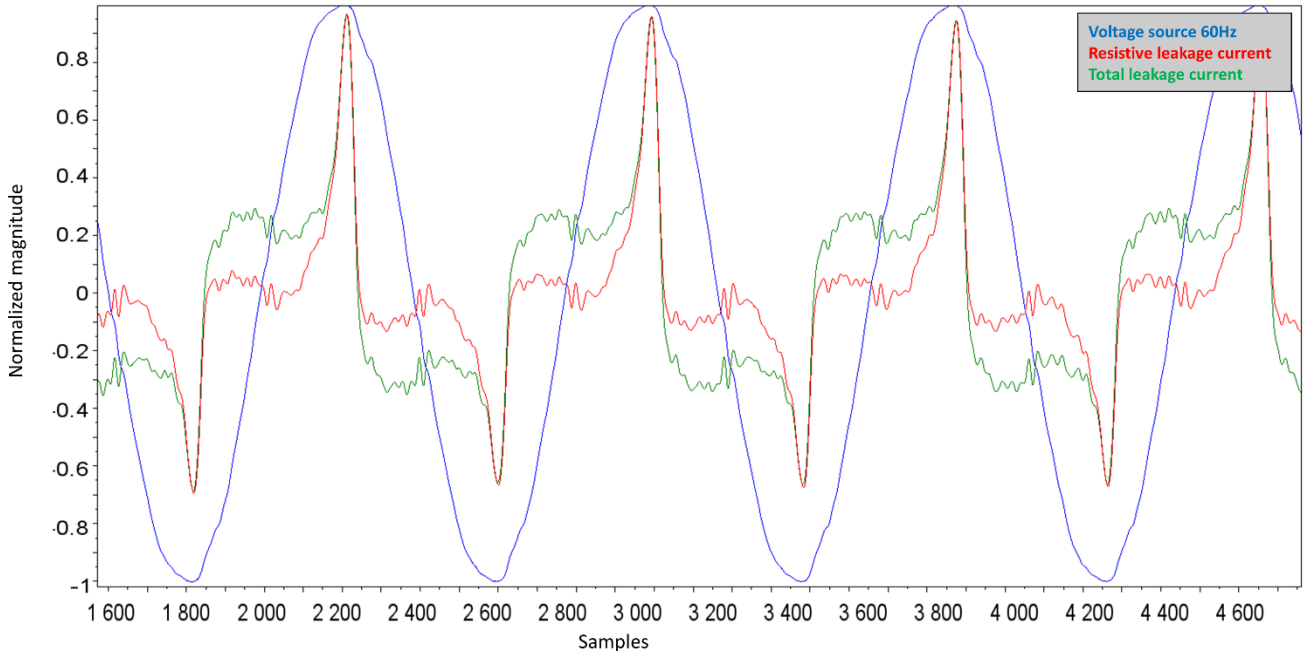

Figure 13. Asymmetry leakage current arrester PR-9.

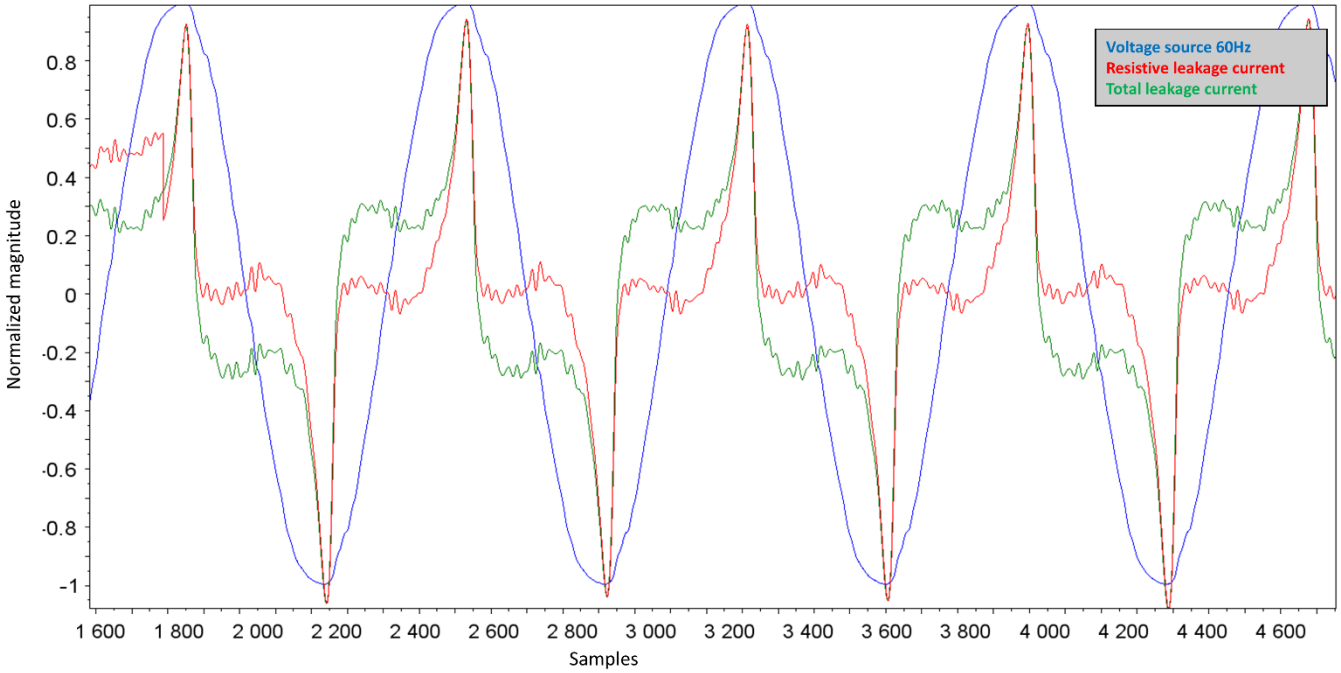

Figure 14. Asymmetry leakage current arrester PR-12.

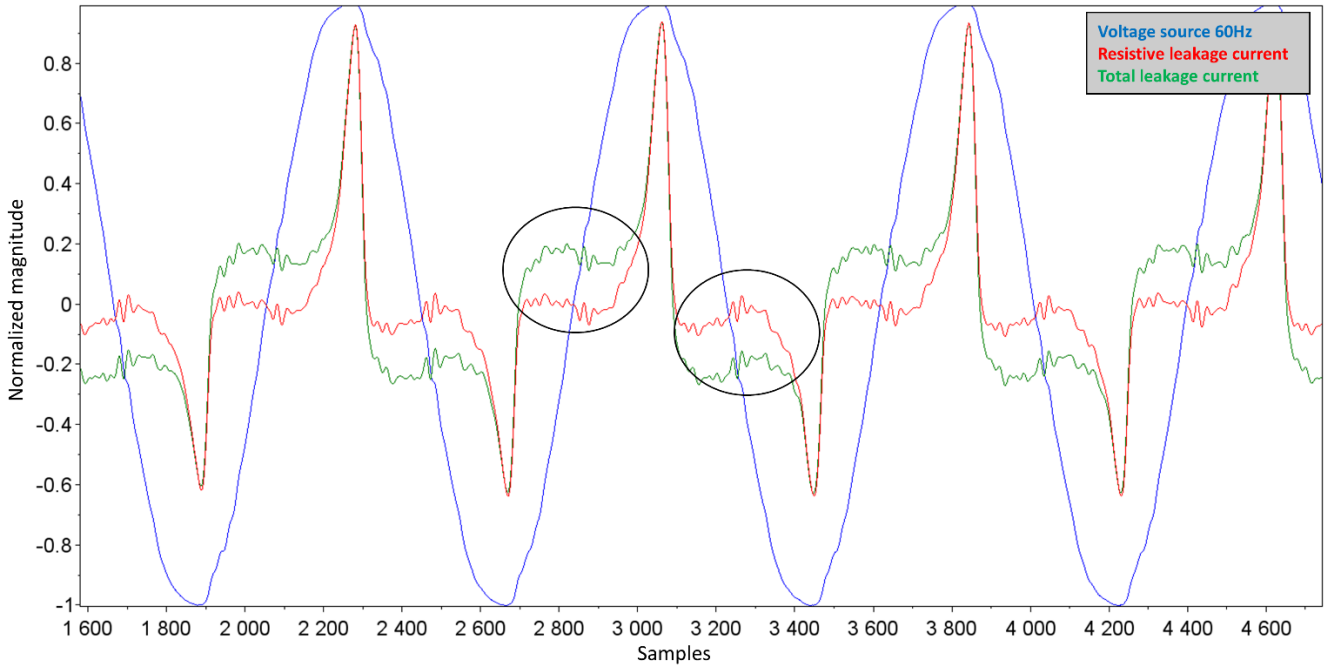

Figure 15. Asymmetry leakage current arrester PR-13.

CONCLUSION

The detection of incipient failures is the objective of the predictive maintenance field. Identifying the predisposition of a surge arrester to failure in the face of future disturbances ensures the reliability of the system it is intended to protect. This article presents the development of a laboratory for conducting aging tests on low-voltage zinc oxide surge arresters. The current waveform impulses applied in the laboratory are sufficient to induce degradation in the electrical parameters of the tested surge arresters. The impulse test conducted in the laboratory allowed for the observation and study of the polarization effects on the surge arrester, evident in the asymmetry between the positive and negative half-cycles of the leakage current.

For future work, the objective is to modify the impulse generator laboratory to allow for higher energy capacity by introducing a capacitor bank charging stage and an additional discharge excitation mechanism. Due to the compact nature of the laboratory, the structure will need to be altered to enhance its dielectric

rigidity to withstand higher voltage levels, enabling its use with medium-voltage surge arresters. This modification requires further studies to ensure the structural changes maintain the mobility capabilities of the laboratory while ensuring safety and efficiency.

Funding: This paper presents part of the results obtained during the execution of the R&D project of code PD-06491-0509/2018 titled “LIGHTNING ROD DETERIORATION MONITORING SYSTEM,” executed by the Gnarus Institute for Copel Geração e Transmissão S.A., the project’s financier, under the Research and Development Program of the Brazilian Electric Sector, regulated by the National Electric Energy Agency—ANEEL.
Conflicts of Interest: The authors declare no conflict of interest.

REFERENCES

1. He J, Lin J, Liu W, Wang H, Liao Y, Li S. Structure-Dominated Failure of Surge Arresters by Successive Impulses. IEEE TransPower Del. 2017 Aug; 32(4):1907-14. doi: 10.1109/TPWRD.2016.2597191.
2. Jiang A, Fu Z, Sun W, Chen J, Wang G, Li R. Experimental and analytical studies of the effects of multiple lightning impulse currents on metal-oxide arrester blocks. Proceedings of the 2014 International Conference on Lightning Protection; 2014 Oct 11-18; Shanghai, China. Piscataway (NJ): IEEE; c2014. p. 681-687, doi: 10.1109/ICLP.2014.6973210.
3. Mardira KP, Saha TK, Sutton RA. Investigation of diagnostic techniques for metal oxide surge arresters. IEEE Trans Diel Elect Ins. 2005 Feb; 12(1):50-9. doi: 10.1109/TDEI.2005.1394015.
4. He J, Zeng R, Chen S, Tu Y. Thermal Characteristics of High-Voltage Whole-Solid-Insulated Polymeric ZnO Surge Arrester. IEEE Power Eng Rev. 2008; 22(10):62. doi:10.1109/mper.2002.4311760.
5. Stojanović ZN, Stojković ZM. Evaluation of MOSA condition using leakage current method. Int J Elec Pow Ener Syst. 2013 Nov; 52:87-95. doi: 10.1016/j.ijepes.2013.03.027.
6. Fujiwara Y, Shibuya Y, Imataki M, Nitta T. Evaluation of Surge Degradation of Metal Oxide Surge Arrester. IEEE Trans Power App Syst. 1982 Apr; PAS-101(4):978-85. doi: 10.1109/TPAS.1982.317164.
7. Tominaga S, Shibuya Y, Fujiwara Y, Imataki M, Nitta T. Stability and Long Term Degradation of Metal Oxide Surge Arresters. IEEE Trans Power App Syst. 1908 Jul; PAS-99(4): 1548-56. doi: 10.1109/TPAS.1980.319580.
8. Seyyedbarzegar SM, Mirzaie M. Thermal balance diagram modelling of surge arrester for thermal stability analysis considering ZnO varistor degradation effect. IET Gener Transm Distrib. 2016; 10:1570-81. doi: 10.1049/iet-gtd.2015.0728.
9. Chrzan KL. Influence of moisture and partial discharges on the degradation of high-voltage surge arresters. Euro. Trans Electr Power. 2004, 14:175-84. doi: 10.1002/etep.15.
10. Brito VS, Lira GRS, Costa EG, Maia MJA. A Wide-Range Model for Metal-Oxide Surge Arrester. IEEE Trans Power Del. 2018 Feb; 33(1):102-109. doi: 10.1109/TPWRD.2017.2704108.
11. Sakshaug EC. A brief history of AC surge arresters. IEEE Power Eng Rev. 1991 Aug; 11(8):11-3. doi: 10.1109/39.90777.
12. Abdul-Malek Z, Yusoff N, Mohd Yousof MF. Field experience on surge arrester condition monitoring - Modified Shifted Current Method. Proceedings of the 45th International Universities Power Engineering Conference. 2010 Aug 31 – Sep 03. Cardiff, UK. Piscataway (NJ): IEEE; c2010. p. 1-5.
13. Munir A, Abdul-Malek Z, Arshad RN. Resistive component extraction of leakage current in metal oxide surge arrester: A hybrid method, Measurement. 2021; 173:108588. https://doi.org/10.1016/j.measurement.2020.108588.
14. Das S, Ghosh R, Dalai S, Chatterjee B. Study on the effect of moisture ingression into metal oxide surge arrester using leakage current analysis. Proceedings of the 2017 3rd International Conference on Condition Assessment Techniques in Electrical Systems. 2017 Nov 16-18. Rupnagar, India. Piscataway (NJ): IEEE; c2017. p. 330-4. doi: 10.1109/CATCON.2017.8280239.
15. Barbosa VRN, Costa EG, Leite Neto AF, Carvalho IF, Castro PF, Souza JPC, et al. Evaluation of the metal oxide surge arresters degradation based on the loss tangent. Proceedings of the IET Conference Proceedings. 2021 Nov 21-26. Xi'an, China. London: IET; c2021. p. 859-64. doi: 10.1049/icp.2022.0089.
16. Nogueira TA, de Salles C, Wanderley Neto ET, Pinheiro FF. Short duration current impulse waveform effects on the degradation and energy absorption capability of zinc oxide varistors. Elec Pow Syst Res. 2023; 220:109336. doi: 10.1016/j.epsr.2023.109336.
17. Ganesh KS. A Review of Zinc Oxide Varistors for Surge Arrester. Proceedings of the 4th International Conference on Electrical Energy Systems. 2018 Feb 7-9. Chennai, India. Piscataway (NJ):IEEE; c2018. p. 470-4. doi: 10.1109/ICEES.2018.8443207.
18. Montenegro JC, Ramirez JL. Degradation of zinc oxide varistors. Proceedings of the First International Caracas Conference on Devices, Circuits and Systems. 1995 Dec 12-14. Caracas, Venezuela. Piscataway (NJ): IEEE; c1995. p. 352-4. doi: 10.1109/ICCDCS.1995.499175.
19. ABB. Blown Out Surge Arrester [Internet]. 2007. Available from: https://megger.com/blog/may-2021/5-facts-about-surge-arresters.
20. Kan M, Nishiwaki S, Sato T, Kojima S, Yanabu S. Surge Discharge Capability and Thermal Stability of a Metal Oxide Surge Arrester. IEEE Trans Power App Syst. 1983 Feb; PAS-102(2): 282-9. doi: 10.1109/TPAS.1983.317765.

21. Holtzhausen K, Vosloo W. High Voltage Engineering Practice and Theory. Netherlands: BSP Books Pvt. Ltd.; 2003. 157 p.
22. Lundquist J, Lennerhag O. Minimum Voltage-Current Characteristic for Calculating Surge Arrester Energy Dissipation in Temporary Overvoltage Conditions. IEEE Trans Power Del. 2022 Jun; 37(3):2268-74. doi: 10.1109/TPWRD.2021.3108841.
23. Carlson WG, Gupta TK, Sweetana A. A Procedure for Estimating the Lifetime of Gapless Metal Oxide Surge Arresters for AC Application. IEEE Trans Power Del. 1986 Apr; 1(2):67-74. doi: 10.1109/TPWRD.1986.4307935.
24. Singh RP, Singh TVP. Influence of pollution on the performance of metal oxide surge arresters. Proceedings of the IEEE Canadian Conference on Electrical and Computer Engineering. 2002 May 12-15. Winnipeg, Canada. Piscataway (NJ): IEEE; c2002.p. 224-9. doi: 10.1109/CCECE.2002.1015206.
25. Feser K, Kohler W, Qiu D, Chrzan K. Behaviour of zinc oxide surge arresters under pollution. IEEE Trans Power Del. 1991 Apr; 6(2):688-95. doi: 10.1109/61.131128.
26. ABB. Surge Arrester Buyers Guide PEXLIM/EXLIM [Internet]. 2010. Available in: http://www02.abb.com/br, Produtos & Serviços, Produtos de Alta Voltagem (EN).
27. Qiao X, Zhang Z, Sundararajan R, Jiang X, Hu J, Fang Z. The failure arc paths of the novel device combining an arrester and an insulator under different pollution levels. Int J Elect Pow Ener Syst. 2021; 125:106549. doi: 10.1016/j.ijepes.2020.106549.
28. Das AK, Dalai S, Chatterjee B. An Experimental Study to Investigate the Condition of Metal Oxide Surge Arrester under Polluted Environment. Proceedings of the 1st International Conference for Convergence in Engineering. 2020 Sep 5-6. Kolkata, India. Piscataway (NJ): IEEE; c2020. p. 175-9, doi: 10.1109/ICCE50343.2020.9290743.
29. Latiff NAA, Illias HA, Bakar AHA, Dabbak SZA. Measurement and Modelling of Leakage Current Behaviour in ZnO Surge Arresters under Various Applied Voltage Amplitudes and Pollution Conditions. Energies. 2018; 11(4):875. doi: 10.3390/en11040875.
30. Das AK, Dey D, Chatterjee B, Dalai S. A Transfer Learning Approach to Sense the Degree of Surface Pollution for Metal Oxide Surge Arrester Employing Infrared Thermal Imaging. IEEE Sensors J. 2021 Aug; 21(15):16961-8. doi: 10.1109/JSEN.2021.3079570.
31. Da Silva DA, Costa ECM, Franco JL, Antonionni M, Buontempo RC, Abreu SR, et al. Reliability of directly-molded polymer surge arresters: Degradation by immersion test versus electrical performance. Int J Elect Power Ener Syst. 2013 Dec; 53(1):488–98. doi: 10.1016/j.ijepes.2013.05.023.
32. Śmietanka H, Ranachowski P, Ranachowski Z, Wieczorek K, Kudela S. Effects of Degradation in Textolite Elements of Damaged Surge Arresters. Energies. 2022; 15:3643. https://doi.org/10.3390/en15103643.
33. Wang M-H, Hu K-A, Zhao B-Y, Zhang N-F. Degradation phenomena due to humidity in low voltage ZnO varistors. Ceramics Int. 2007 Mar; 33(2):151-4. doi: 10.1016/j.ceramint.2005.08.009.
34. IEC 60060-1. High Voltage Test Techniques, Part 1, General Definition and Test Techniques. Geneva, Italy. 1994. 78 p.
35. Hauschild W, Lemke E. High-Voltage Test and Measuring Techniques. Dresden: Springer; 2014. 518 p.
36. Edwards FS, Husbands AS, Perry FR. The development and design of high-voltage impulse generators. Proc IEE - Part I: General. 1951; 98(111)155-68. doi: 10.1049/pi-1.1951.0054.

© 2024 by the authors. Submitted for possible open access publication under the terms and conditions of the Creative Commons Attribution (CC BY NC) license (https://creativecommons.org/licenses/by-nc/4.0/).